

Signatures of chronic pain in multiple sclerosis: a machine learning approach to investigate trigeminal neuralgia

Timur H. Latypov^{a,b,c}, Abigail Wolfensohn^{a,b,d}, Rose Yakubov^{a,e}, Jerry Li^{a,b,c}, Patcharaporn Srisaikaew^a, Daniel Jörgens^a, Ashley Jones^f, Errol Colak^g, David Mikulis^{a,h}, Frank Rudzicz^{i,j}, Jiwon Oh^{b,f}, Mojgan Hodaie^{a,b,k,*}

Abstract

Chronic pain is a pervasive, disabling, and understudied feature of multiple sclerosis (MS), a progressive demyelinating and neurodegenerative disease. Current focus on motor components of MS disability combined with difficulties assessing pain symptoms present a challenge for the evaluation and management of pain in MS, highlighting the need for novel methods of assessment of neural signatures of chronic pain in MS. We investigate chronic pain in MS using MS-related trigeminal neuralgia (MS-TN) as a model condition focusing on gray matter structures as predictors of chronic pain. T1 imaging data from people with MS ($n = 75$) and MS-TN ($n = 77$) using machine learning (ML) was analyzed to derive imaging predictors at the level of cortex and subcortical gray matter. The ML classifier compared imaging metrics of patients with MS and MS-TN and distinguished between these conditions with 93.4% individual average testing accuracy. Structures within default-mode, somatomotor, salience, and visual networks (including hippocampus, primary somatosensory cortex, occipital cortex, and thalamic subnuclei) were identified as significant imaging predictors of trigeminal neuralgia pain. Our results emphasize the multifaceted nature of chronic pain and demonstrate the utility of imaging and ML in assessing and understanding MS-TN with greater objectivity.

Keywords: Machine learning, Chronic pain, Multiple sclerosis, Trigeminal neuralgia, Brain imaging

1. Introduction

Chronic pain is a leading cause of disability worldwide,¹⁷ exerting a massive burden on both individuals and society. Experiencing chronic pain can affect all aspects of a person's life, putting

a major strain on their mental health and ability to perform daily tasks.²⁵ Specific populations may experience difficulty in self-report of pain, such as those with motor or cognitive limitations or advanced stages of neurological disorders.²⁰

Among these disorders, multiple sclerosis (MS) is particularly noteworthy as it has a high prevalence of chronic pain and affects approximately 50% to 75% of MS population.^{15,44,51} Chronic pain, however, has remained largely unaddressed in assessments of disability in MS. Importantly, the expanded disability status scale, the standard scale used to evaluate the magnitude of neurological disability, does not explicitly include chronic pain.²⁸ This underscores the need for and importance of investigating novel chronic pain markers for patient care, advocacy, and improvement of patients' quality of life.

Current literature in neuroimaging links chronic pain to abnormalities in brain structure and function, particularly in gray matter (GM) morphology.^{1,8,52} Multimodal imaging studies suggest that these structures potentially can be used as the objective signatures for chronic pain.^{1,8,31} However, the relationship between GM abnormalities and pain was not studied in MS. Although MS is a disease that primarily affects white matter, diffuse neurodegeneration and the presence of myelin in GM render patients with MS also susceptible to GM alterations.^{18,29,54,55} Therefore, investigation of relationship between pain in MS and GM is particularly relevant and may pave the way towards clearer imaging biomarkers of pain.

The case of patients with trigeminal neuralgia (TN) illustrates the severe impact of such pain conditions. Trigeminal neuralgia is characterized by intense, electric shock-like pain episodes that usually occurs unilaterally.⁴⁹ TN has been described as one of the most severe types of pain human can experience.⁶⁰ Moreover,

Sponsorships or competing interests that may be relevant to content are disclosed at the end of this article.

^a Division of Brain, Imaging and Behaviour, Krembil Research Institute University Health Network, Toronto, ON, Canada, ^b Institute of Medical Science, Temerty Faculty of Medicine, University of Toronto, Toronto, ON, Canada, ^c Collaborative Program in Neuroscience, University of Toronto, Toronto, ON, Canada, ^d Faculty of Science, McGill University, Montreal, QC, Canada, ^e MD Program, Temerty Faculty of Medicine, University of Toronto, Toronto, ON, Canada, ^f Division of Neurology, Department of Medicine, St. Michael's Hospital, Unity Health Toronto, Toronto, ON, Canada, ^g Department of Medical Imaging, St. Michael's Hospital, Unity Health Toronto, Toronto, ON, Canada, ^h Joint Department of Medical Imaging, Toronto Western Hospital, University Health Network, Toronto, ON, Canada, ⁱ Vector Institute for Artificial Intelligence, Toronto, ON, Canada, ^j Faculty of Computer Science, Dalhousie University, Halifax, NS, Canada, ^k Department of Neurosurgery, Toronto Western Hospital, University Health Network, Toronto, ON, Canada

*Corresponding author. Address: Department of Neurosurgery, Toronto Western Hospital, University Health Network, 399 Bathurst St, 4-443, Toronto, ON M5T2S8, Canada. Tel.: +1(416)603-6441. E-mail address: mojan.hodaie@uhn.ca (M. Hodaie).

Supplemental digital content is available for this article. Direct URL citations appear in the printed text and are provided in the HTML and PDF versions of this article on the journal's Web site (www.painjournalonline.com).

Copyright © 2024 The Author(s). Published by Wolters Kluwer Health, Inc. on behalf of the International Association for the Study of Pain. This is an open access article distributed under the terms of the Creative Commons Attribution-Non Commercial-No Derivatives License 4.0 (CCBY-NC-ND), where it is permissible to download and share the work provided it is properly cited. The work cannot be changed in any way or used commercially without permission from the journal.

<http://dx.doi.org/10.1097/j.pain.0000000000003497>

TN has a high degree of comorbidity with MS; people with MS develop TN at a 20-fold greater rate than the general population.¹² This trend has led to the classification of a unique subtype of TN known as TN secondary to MS (MS-TN), emphasizing complex relationship between MS and severe pain syndromes.¹⁹

Recent advances in machine learning (ML) present an opportunity to investigate these relationships. Machine learning is increasingly being used in neuroimaging, allowing for more nuanced analyses data, compared to conventional univariate statistical approaches.⁶ Previously, ML had been successfully applied to various data modalities (structural/functional imaging, positron emission tomography) and tasks for investigating chronic pain, including identifying imaging predictors for trigeminal pain and its surgical treatment outcome.^{21,23,31,34,50} Notably, ML can consider the larger interactions between variables rather than rely on univariate comparisons.^{3,6} This advantage may be especially relevant to the study of the brain because of the high numbers of biological variables and prevalence of structural and functional connections between regions or variability in magnetic resonance imaging (MRI) acquisition protocols.^{3,13,46}

In this study, we sought to identify GM signatures of chronic pain in people with MS using ML and MS-TN as a model condition. We hypothesise that GM metrics drawn from MRI data can provide accurate individual-level insights about chronic pain in MS.

2. Materials and methods

2.1. Ethics

This retrospective study was reviewed and approved by the research ethic boards of the University Health Network (UHN) and Unity Health Toronto. As patient data included in the study was collected retrospectively, additional informed consent was not required according to the institutional Research Ethics Board policy.

2.2. Participants

Patients with MS from the Barlo MS clinic at St. Michael's Hospital and patients with TN from the Toronto Western Hospital (TWH) (followed-up between 2010 and 2023) were screened for this retrospective study. Patients with TN were considered for inclusion if they met the diagnostic criteria for MS-TN as defined by the International Classification of Headache Disorders third Edition (13.1.1.2.1).¹⁹ For the purpose of the current study, we restricted the pool of participants to those that have MS-TN and sufficient cognitive ability to describe details about their pain history and symptomatology. Patients with comorbidities such as Alzheimer, Parkinson disease, brain tumours, other chronic pain conditions or other neurodegenerative disorders were excluded.

We matched MS-TN group (TWH) participants with MS identified from the Barlo MS Centre clinic registry by sex, age, and the duration of their MS. Barlo MS Centre cohort included patients with no history of chronic pain. Every participant had retrospectively acquired T1-weighted (T1w) structural brain imaging performed in a 3 T MRI scanner. Details on datasets are outlined in **Table 1**.

2.3. Cortical and subcortical gray matter segmentation and feature extraction

The T1w imaging data of each patient was processed using the *recon-all* pipeline of FreeSurfer 7.2.¹⁶ Previously, this framework

was successfully used for predicting surgical outcome in TN and distinguishing TN from healthy controls (HCs).^{23,31} In addition, this pipeline shown to be agnostic for the MRI scanner difference.^{31,42}

We ran data processing on Lenovo SD530 servers (Intel Xeon SP Skylake, Linux CentOS 7.9). Using *recon-all* pipeline, we obtained cortical surface area and thickness measures from 148 cortical regions defined by the Destrieux atlas in each subject.¹¹ Regional subcortical volume of the hippocampus, amygdala, and thalamus were also extracted, along with the estimated total intracranial volume (**Fig. 1A**). Within the cortex, surface area and thickness were extracted as individual metrics because doing so has been shown to yield more precise results than extracting cortical volume alone.⁵⁸ If brain images could not be successfully parcellated by FreeSurfer (because of error or inaccurate segmentation), they were excluded from analysis. FreeSurfer output was screened for artifacts and errors.

All extracted measures were corrected for individual variations in head size in accordance with previous imaging studies^{23,31} using formula:

$$GM_{corr} = \frac{GM_{raw}}{eTIV}$$

where GM_{raw} —the uncorrected size (thickness/volume/area) of GM region, $eTIV$ —estimated total intracranial volume of subject (computed by FreeSurfer), and GM_{corr} —corrected size (thickness/volume/area) of GM region. In total, 410 metrics, including 148 cortical thickness, 148 cortical surface area (296 cortical vertex-based measures), and 114 subcortical volume metrics (voxel-based measures), were extracted and analysed using a combination of unsupervised and supervised ML methods.

2.4. Unsupervised machine learning

We applied t-distributed stochastic neighbor embedding (t-SNE) to the extracted GM metrics. This approach allows to reduce dimensionality of data from 410 to 2 and easily visualize the multidimensional imaging dataset structure and possible clusters. t-SNE analysis was performed to inspect imaging data and assess whether the data would get clustered based on factors such as scanner differences, clinical, and demographic variables (sex, age, diagnosis). Using this approach, we can disregard potential skewness of entire dataset. We used t-SNE perplexity parameters of 5 and Z-score normalization of the entire dataset. The t-SNE algorithm from the *Python* library Scikit-learn 1.2.1⁴⁷ was used.

2.5. Supervised machine learning pipeline

We constructed a supervised ML model using Scikit-learn with the goal of training it to distinguish between the MS and MS-TN GM imaging metrics. We used a support vector machine (SVM) classifier with linear kernel (Parameters: C-value = 0.01, Gamma—"scaled," tol=0.001, "class_weight"—"balanced"). Parameters were based on literature and previous reports.^{4,23,38,39} SVM was chosen due to its ability to classify multidimensional data. We used linear kernel for separating 2 classes as it allows to extract coefficients of SVM and evaluate important features. "Tol" and "gamma" parameters (tolerance for stopping the training and kernel coefficient respectively) were using default values. C value of 0.01 (regularization parameter) was chosen to increase the margin of decision boundary for SVM.⁴ Before training the model, we applied Pearson Redundancy Based Filter (correlation threshold = 0.9) to remove highly correlated features.⁵

To train and test the model, we used sequential backwards feature selection from the MLXtend *Python* package⁴⁵ using

Table 1
Datasets and acquisition parameters.

Dataset	Scanner	Acquisition parameters
MS-TN (UHN)	3T GE Signa HDx	T1w: matrix = 256 × 256, flip angle = 20°, FOV = 24 cm, voxel size = 0.94 × 0.94 × 1 mm
	3T Siemens Vida	T1w: matrix = 256 × 256, flip angle = 9°, FOV = 25.6 cm, voxel size = 1 × 1 × 1 mm
MS (Unity Health)	3T Siemens TIM trio	T1w: matrix = 256 × 240, flip angle = 9°, FOV = 25.6 cm, voxel size = 1 × 1 × 1 mm
HC (CamCAN)	3T Siemens TIM trio	T1w: matrix = 256 × 240, flip angle = 9°, FOV = 25.6 cm, voxel size = 1 × 1 × 1 mm

CamCAN, Cambridge Centre for Ageing Neuroscience; FOV, field of view; GE, general electric; HC, healthy control; MS, multiple sclerosis; T1w, T1-weighted; TIM, total imaging matrix; TN, trigeminal neuralgia; UHN, University Health Network.

stratified 10-fold nested cross-validation, to ensure generalizability on the unseen data (Supplementary material 1, <http://links.lww.com/PAIN/C188>). The imaging dataset was divided into 10 folds, and the model underwent training and testing 10 times: one fold acted as the test fold, while the remaining 9 were used to perform the feature selection and train the model. After selecting optimal set of features on inner folds, we trained the final model and assessed it using out-of-sample test subset of cross-validation. This allowed us to use all the data to test the model, optimize set of predictors on nested training folds, and avoid any possible data leakage. Z-score normalization was applied to training and testing subsets of data, with mean and standard deviation values estimated based on training subset. **Figure 1B** illustrates the data analysis framework.

Model accuracy (% correct predictions) and the area under the receiver operating characteristic (ROC) curve, as well as the confusion matrix, were reported. For each testing fold, we extracted a set of predictive features and their corresponding SVM feature weights. These features were used for subsequent statistical analysis.

2.6. Univariate statistical analysis

We tested sets of important predictors derived from the SVM model using an independent *t* test to identify the directionality of changes between MS and MS-TN groups. To ensure consistency and generalizability, only features that were selected at least 5 out of 10 times during the cross-validation procedure were chosen for the univariate analysis. χ^2 test was used to compare proportions of males/females and types of MS in datasets. All *P*-values were corrected for multiple comparisons using the false discovery rate procedure (Benjamini–Hochberg).

We analyzed data from age- and sex-matched HCs to confirm the directionality of regional structural changes between the MS/MS-TN population. Cambridge Centre for Ageing Neuroscience

dataset was used as a source of HC data.⁵³ Previous study confirmed that this dataset is highly similar to the UHN cohort and does not require harmonization (**Table 1**).³¹

3. Results

3.1. Participant demographics

A total of 916 patients with TN and 200 people with MS were screened. Based on inclusion/exclusion criteria, we identified 80 MS-TN subjects for analysis. These subjects were matched by age, sex, and duration of MS with 80 subjects with MS but without a diagnosis of TN from the Barlo MS Centre clinic registry (Supplementary material 2, <http://links.lww.com/PAIN/C188>). We excluded subjects who had a lack of T1w imaging or those with failed data extraction (*recon-all* error) because of artifacts. A total of 152 patients were studied with a mean age of 54.37 ± 9.10 years (MS) and 55.38 ± 9.88 years (MS-TN); mean duration of MS was 16.69 ± 9.52 years (MS) and 16.44 ± 9.98 years (MS-TN) (**Table 2**). As 8 subjects (5 MS and 3 MS-TN subjects) were excluded because of the failed *recon-all* pipeline, the final dataset matching is not 1:1. However, no statistically significant difference was found in the proportion of male/female subjects ($\chi^2 P > 0.05$), age (*t* test $P > 0.05$), and duration of MS between groups (*t* test $P > 0.05$). Patients with relapsing–remitting, primary progressive, and secondary progressive MS were included in both groups. Ten subjects (8 from MS-TN group and 2 from MS group) had no information about the type of the MS at the time of follow-up; however, for the remaining subjects, no statistically significant difference was found in the proportion of different types of MS ($\chi^2 P > 0.05$). Participants from both groups used disease modifying medications, including natalizumab, teriflunomide, and interferon-beta agents. In addition to these, MS-TN participants were actively using neuropathic pain medication, including gabapentin, carbamazepine, and pregabalin. Among the patients with MS-TN, the mean duration of TN pain was 5.39 ± 4.60 years. A total of 36 of

Table 2
Demographic information on study population.

Condition	MS	MS-TN	HC
Age (y)	54.37 ± 9.10	55.38 ± 9.88	55.38 ± 9.88
Sex	F = 47, M = 28	F = 45, M = 32	F = 45, M = 32
Types of MS	RR = 47, PP = 18, SP = 8, N/A = 2	RR = 35, PP = 23, SP = 11, N/A = 8	N/A
Duration of MS (y)	16.69 ± 9.52	16.44 ± 9.98	16.44 ± 9.98
Duration of TN pain (y) (MS-TN only)	N/A	5.39 ± 4.60	N/A
Side of pain (MS-TN only)	N/A	L = 36; R = 37; Bilateral = 4	N/A

HC, healthy control; MS, multiple sclerosis; PP, primary progressive; RR, relapsing–remitting; SP, secondary progressive; TN, trigeminal neuralgia.

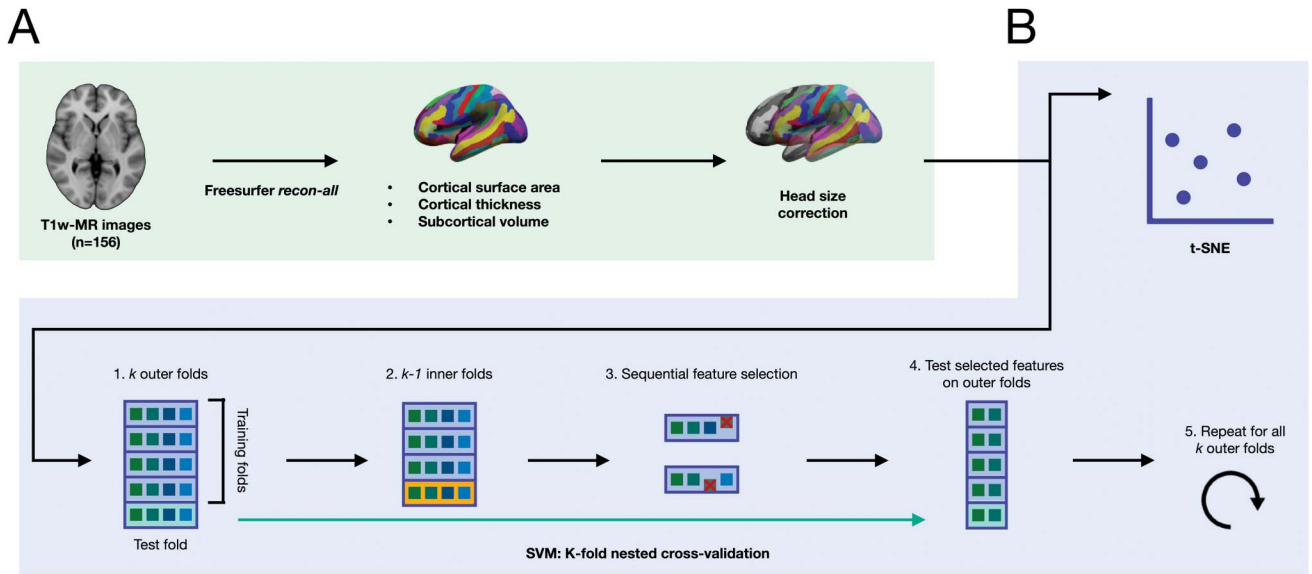


Figure 1. Data processing and analysis pipeline. Magnetic resonance imaging (MRI) data were processed using FreeSurfer (A), gray matter metrics were corrected for the difference in head size and used for the ML-driven analysis. Machine learning pipeline (B) includes unsupervised (t-SNE) and supervised (SVM) ML components and illustrates nested cross-validation scheme for training, optimising, and testing model. ML, machine learning; SVM, support vector machine; t-SNE, t-distributed stochastic neighbor embedding.

the patients with MS-TN were experiencing left-sided pain, 37 were experiencing right-sided pain, and 4 were experiencing bilateral (both left and right-sided) pain.

3.2. Unsupervised machine learning illustrates data structure

The clustering algorithm was applied to all 410 features and demonstrated the data structure with respect to diagnosis, scanner model, duration of the patients’ MS, or age. We confirmed that the imaging data are suitable for subsequent analysis with supervised ML. Specific demographic, clinical, and imaging covariates did not result in data clustering, or skewness. Notably, scanner model does not result in clear clustering of data

points, which is consistent with previous observations on GM metrics.^{31,42} We, therefore, expect that the subsequent ML results are unlikely to be biased towards the above covariates. The results of applying t-SNE to the data are shown in **Figure 2**.

3.3. Supervised machine learning accurately distinguishes multiple sclerosis and multiple sclerosis-trigeminal neuralgia

The binary classification model (SVM) was trained across all 10 folds of cross-validation with feature selection identifying the optimal set of imaging predictors (min of 14 features, max of 35 features). The model had an average train accuracy of $99.5 \pm 0.5\%$ and average test accuracy of $93.4 \pm 5.9\%$ over the 10 folds with an

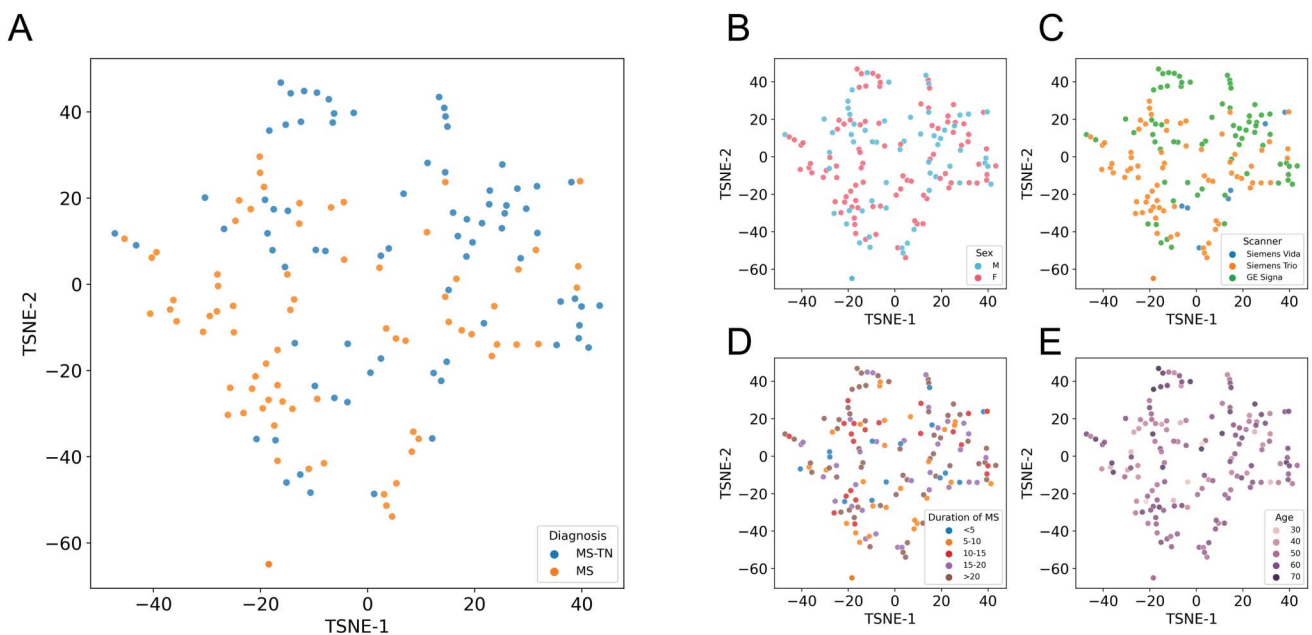


Figure 2. T-distributed stochastic neighbor embedding (t-SNE) clustering of the data (perplexity = 5), where each point represents a different patient from the dataset and the hue in each of the 4 subplots, corresponds to different variables that were tested because of their potential to be confounders. (A) Diagnosis, (B) sex, (C) scanner, (D) duration of MS in years, and (E) age (decades). The axes on each subplot are arbitrary. MS, multiple sclerosis.

area under the ROC curve of 0.98 ± 0.6 . The SVM classifier accurately predicted both MS and MS-TN at similar rates (0.95 and 0.92 for MS and MS-TN, respectively). A summary of the model's average performance is highlighted in **Figures 3A and B**.

The model consistently identified a set of 17 features across 16 cortical and subcortical GM regions as highly predictive of the presence of TN pain in people with MS. This included metrics from thalamic subnuclei (right ventral medial nucleus volume, left ventral posterolateral nucleus volume, right medial mediodorsal nucleus volume, left pulvinar inferior nucleus volume, right limitans supragenulate nucleus volume), hippocampal regions (right CA3 body volume), the insula (left and right inferior circular sulci thickness), frontal regions (left gyrus rectus [RG] thickness, right superior frontal sulcus [SUPFS] area), parietal regions (right postcentral gyrus area), temporal regions (right Heschl gyrus area, right fusiform gyrus area), occipital regions (right cuneus [CUN] thickness, left superior occipital sulcus and transverse

occipital sulcus [TOS] area), and other regions (left pericallosal sulcus [PERCAS] area and thickness) (**Fig. 3C**).

Top imaging predictors derived by the model represent 5 brain networks delineated in Uddin et al.'s⁵⁶ functional atlas. Structures from default-mode, somatomotor, visual, salience, and control networks were shown as important for distinguishing between MS and MS-TN. Six of the top features across 4 cortical regions represent sulci of Destrieux atlas. These structures are forming the boundaries across GM nodes; therefore, they were not classified into functional networks.

3.4. Post-hoc statistics demonstrate differences in gray matter

An independent *t* test was applied to the 17 features selected by the supervised ML model during at least 5 of the 10 folds (**Fig. 3C**). Analysis revealed that right hippocampal CA3 body volume, right

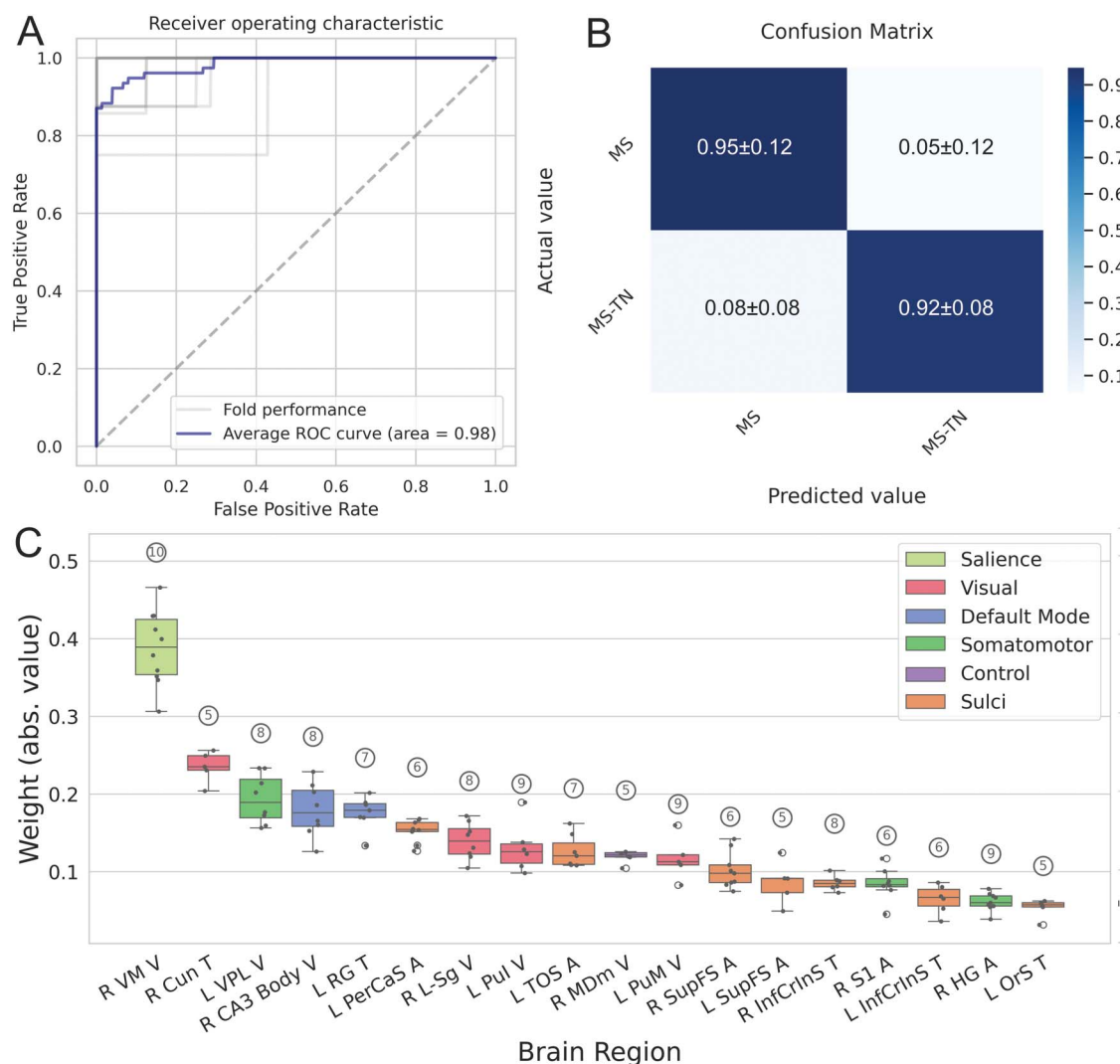


Figure 3. Average receiver operating characteristic (ROC) curve of individual point-wise predictions (A and B) confusion matrix visualizing the total performance of the model. The average area under the ROC curve is 0.98, indicating that the model is correctly categorizing the data significantly higher than random chance; the dotted line illustrates a random sorting curve, and the gray curves show performance of individual folds. (C) Top features according to the weight attributed by the SVM classifier. Y-axis represents unitless feature importance (coefficient), assigned to it by the SVM model. Features were included if selected by the model during at least 5 of the 10 cross-validation folds of training; the number in the circle above each feature represents the number of times out of 10 it was selected. Features are coloured according to the specific brain network—default mode, somatomotor, salience, control, visual networks, and gyral structures (not classified). A, area; CUN, cuneus; FUG, fusiform gyrus; HG, Heschl gyrus; INFCRINS, inferior circular sulci of the insula; L, left hemisphere; L-SG, limitans supragenulate thalamic nucleus; MDm, medial mediodorsal thalamic nucleus; Pul, pulvinar inferior thalamic nucleus; PERCAS, pericallosal sulcus; RG, gyrus rectus; R, right hemisphere; S1, postcentral gyrus; SVM, support vector machine; SUPFS, superior frontal sulcus; T, thickness; TOS, superior occipital sulcus and transverse occipital sulcus; V, volume; VM, ventral medial thalamic nucleus; VPL, ventral posterolateral thalamic nucleus.

ventral medial thalamic nucleus volume, left ventral posterolateral thalamic nucleus volume, and right medial mediodorsal thalamic nucleus (MDm) showed significant relative reductions in the MS-TN group compared to MS. Meanwhile, left PERCAS area and thickness, right postcentral gyrus area (S1) right SUPFS area, left superior occipital sulcus and TOS area, left RG thickness, and right CUN thickness showed significant increases in MS-TN compared to MS. Some of these structures were significantly reduced in both MS and MS-TN comparing to HC (R VM, R MDm, R Cun). Changes in right CA3 and left ventral posterolateral thalamic nucleus volumes, left TOS, and right S1 area were observed exclusively in subjects with MS-TN and were not significantly different in pain-free MS group comparing to the HC. **Figure 4** shows the univariate comparison of important predictors derived by ML algorithm.

4. Discussion

Understanding chronic pain is inherently challenging because of the multifaceted biological, psychological, and social components it encompasses. In this study, we investigated whether ML was capable of uncovering signatures of chronic pain in MS, based strictly on imaging data, by comparing 2 MS cohorts—one with TN pain and one without pain. Our analyses revealed that MS-TN is associated with GM alterations within default-mode, somatomotor, salience, and visual network structures. These GM structures were sufficiently different between the cohorts to allow our ML model to predict pain with an individual accuracy of 93.4%. This is a significant step towards the identification of pain biomarkers in MS, allowing for possible new avenues of investigating pain in this group using MRI signatures. Machine learning models are capable of processing data with large sample sizes and vast amounts of variables with greater efficiency, allowing for the comparison of many different subjects and brain regions at once.

4.1. Gray matter signatures of chronic pain

Our ML model identified 17 GM structures important in distinguishing subjects with and without chronic pain in MS and contribute to the pain phenotype in MS-TN.

The CA3 region of the hippocampus, a structure important for memory processing, exhibited volume reductions in the MS-TN group compared to both MS and HC. These results align with previously reported patterns in classical TN.^{40,57} Notably, past research has highlighted the plasticity of the GM within the hippocampus. In patients with TN, GM alterations were found to be reversible; successful surgical interventions led to the normalization of hippocampal volume.⁴⁰ Moreover, abnormalities of hippocampus were shown to be inhomogeneous across subfields.^{40,57} When comparing the MS population with HC, we did not observe hippocampal volume differences, suggesting that the observed hippocampal abnormal volume is closely related to the expression of pain in MS-TN subjects.

Thalamic nuclei have been implicated in pain processing and modulation. The ventral medial thalamus has been described as one of the “discriminators” in the control of nociception.⁵⁹ Reduction of thalamic volume has previously been shown in trigeminal neuropathic pain and chronic pain populations.^{9,31} The reduction in volume and activity of the medial thalamic nuclei, including the ventral medial and mediodorsal nuclei, has been linked to the sensory discriminative and emotional-affective dimensions of pain on both humans and animal models.^{7,22} Our finding suggests that these domains are affected in MS subjects and more prominent in MS-TN group.

Our ML model also pointed to increased cortical areas and thickness in regions such as the PERCAS, postcentral gyrus (S1), and SUPFS. These areas may suggest a compensatory mechanism or maladaptive plasticity associated with chronic pain. Abnormalities in structure and function of primary somatosensory cortex were previously shown in neuropathic pain.^{32,33,48} Increase in thickness was attributed to the higher pain and temperature sensitivity.¹⁴ Structural changes in prefrontal cortex were reported in various chronic pain conditions, including TN, temporomandibular joint disorder, and back pain.^{35,36,41} Interestingly, these abnormalities were shown to be associated with neuroticism and affective components of pain perception.^{35,36}

In the examined cohort, no significant changes were observed in the right Heschl gyrus area, right orbitofrontal cortex thickness,

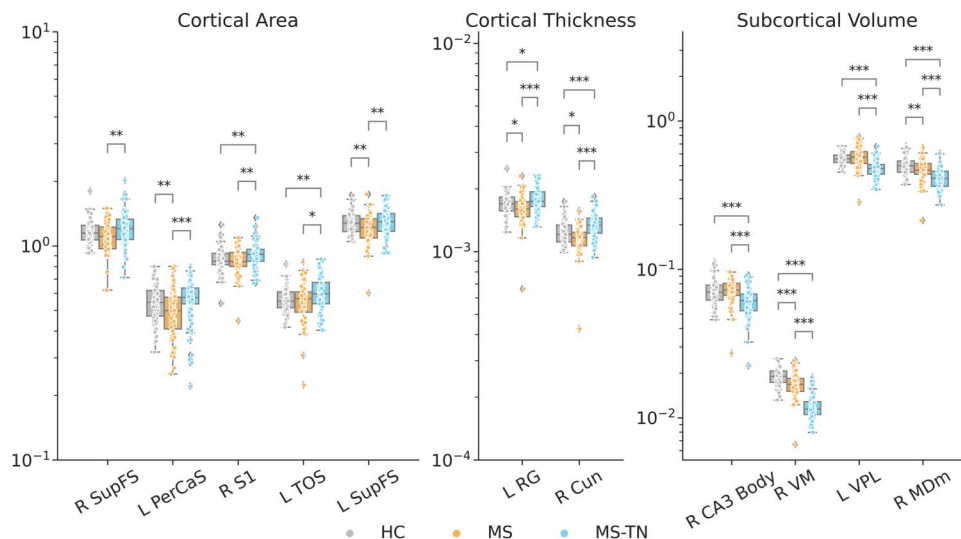


Figure 4. Visualization of the univariate statistics of important predictive features, mapped according to the corrected size of the region in MS-TN (blue) vs MS (orange) patients to assess directionality. Features are organized in terms of the dimension they were selected for, with (A) visualizing cortical surface area, (B) visualizing cortical thickness, and (C) visualizing subcortical volume. The corrected *P*-values are listed above each feature in accordance with the legend on the right, only significant features are displayed (****P* < 0.001, ***P* < 0.01, **P* < 0.05). Log scale is used for visualization. MS, multiple sclerosis; TN, trigeminal neuralgia.

left and right inferior circular sulci of the insula thickness, right supragenicular thalamic nucleus volume, and left pulvinar thalamic nuclei volume across compared groups. However, the lack of significant alterations in these regions does not preclude their potential role as biomarkers, as ML models, in contrast to traditional statistical methods, possess the capability to discern complex interfeature interactions.³⁸ For instance, the insula, with its robust projections from the ventromedial thalamus, and S1—identified as key predictors in the model⁵⁹—this might reflect intricate network dynamics. Moreover, previous studies have noted orbitofrontal cortex alterations in chronic pain patients, which are functionally associated with pain and treatment expectations.^{2,36} Similarly, the CUN gyrus, integral for multisensory integration, exhibits reduction in TN patients compared to HC.⁴³ This suggests that variations in regions such as the RG and CUN could be indicative of more extensive network disruptions in MS-TN.

These results further support the network-level alterations of the human brain in pain, highlighting both the reciprocal modulation of structures and the advantage of data-driven investigation approaches over univariate analyses. There is a great interest in exploring brain networks and their abnormalities as predictors of pain,⁵⁰ and our study demonstrates noninvasive approach to analyzing these networks on a structural level. That is especially relevant in the context of MS as a chronic disorder that has both demyelinating and neurodegenerating components of pathogenesis and may have complex imaging and clinical manifestation, especially in combination with chronic pain.^{24,30,37} Unlike classical TN, which usually affects older individuals without MS, TN in people with MS can occur at a younger age and may have less successful surgical outcomes.^{12,26} These clinical and therapeutic response observations underscore the relevance of pain-specific biomarkers in MS, which would facilitate the ability to provide optimal care for TN in people with MS.

4.2. Limitations

We compared 2 distinct MS-affected populations and used HC to characterise the directionality of changes. We acknowledge that the cross-sectional and retrospective design may limit our ability to fully interpret these changes over time. Longitudinal studies focused on the MS population would be helpful for a greater understanding of dynamic brain abnormalities.

We cannot completely rule out the influence of neuropathic pain medication on the brain morphology. Because of the severity of MS-TN, it is not feasible to investigate medication-free patients; therefore, our analysis reflects typical MS-TN population.

We opted against stratifying all clinical subtypes of MS to maintain a substantial sample size for our ML-driven comparison between MS and MS-TN groups. Moreover, there is accumulating recognition that the current MS disease subtypes are insufficient, and MS is a disease continuum²⁷—therefore, it is likely to be of limited significant to stratify by disease subtype, and more meaningful to match by age, sex, and disease duration, which was done in our study. Our matching criteria between the 2 populations focused on the duration of MS, age, and sex. We ruled out type of MS and possible scanner influence as potential confounding factors influencing prediction. This allowed us to collect a well-curated imaging dataset. Finding a comparable, publicly available dataset that includes data about possible pain-free patients with MS together with detailed clinical annotations has proven to be challenging, particularly because chronic pain is very common in MS (up to 75% affected), but often not recognized. While external validation would be beneficial, the

strength of this work lies in the depth and detail of our unique dataset.

We acknowledge that the usage of FreeSurfer, while offers several advantages (such as automatic pipeline, consistency, and MRI scanner agnostic metrics), might also be the subject to the variation in terms of the segmentation accuracy. This might be prominent in regions, like hippocampus and thalamus, making them challenging to parcellate.¹⁰ We focused solely on imaging metrics as this is the most accurate/reliable way to analyze retrospective data. This approach allowed us to accurately pinpoint structures predominantly affected in MS-TN compared to a demographically similar MS population.

5. Conclusion

Our work highlights the potency of ML algorithms in investigating chronic pain in MS as a multimorbid condition. Machine learning model achieved high (>90%) accuracy in distinguishing MS-TN and MS based on GM metrics alone. The accurate data-driven comparison between pain and nonpain groups among people with MS allows us to derive imaging-based signatures of chronic pain, establishing potential objective GM markers of TN in MS. This study sheds light on a distinct subset of trigeminal pain disorders that is arising from central nervous system exclusively. Investigating the relationship between MS and MS-TN will facilitate a better assessment and treatment of chronic pain conditions in MS, and this study is an important first step in that direction.

Conflict of interest statement

The authors have no conflicts of interest to declare.

Acknowledgements

This research was supported by CIFAR-Temerty Innovation Catalyst Grant, University of Toronto Centre for the Study of Pain and Temerty Faculty of Medicine, University of Toronto.

Data sharing: Code and model will be available upon reasonable request.

Supplemental digital content

Supplemental digital content associated with this article can be found online at <http://links.lww.com/PAIN/C188>.

Article history:

Received 10 May 2024

Received in revised form 30 October 2024

Accepted 1 November 2024

Available online 13 December 2024

References

- [1] Alshelhi Z, Brusaferrri L, Saha A, Morrissey E, Knight P, Kim M, Zhang Y, Hooker JM, Albrecht D, Torrado-Carvajal A, Placzek MS, Akeju O, Price J, Edwards RR, Lee J, Sclocco R, Catana C, Napadow V, Loggia ML. Neuroimmune signatures in chronic low back pain subtypes. *Brain* 2022; 145:1098–110.
- [2] Atlas LY, Wager TD. How expectations shape pain. *Neurosci Lett* 2012; 520:140–8.
- [3] Bakas S, Reyes M, Jakab A, Bauer S, Rempfler M, Crimi A, Shinohara RT, Berger C, Ha SM, Rozycki M, Prastawa M, Alberts E, Lipkova J, Freymann J, Kirby J, Bilello M, Fathallah-Shaykh H, Wiest R, Kirschke J, Wiestler B, Colen R, Kotrotsou A, Lamontagne P, Marcus D, Milchenko M, Nazeri A, Weber MA, Mahajan A, Baid U, Gerstner E, Kwon D, Acharya G, Agarwal

- M, Alam M, Albiol A, Albiol A, Albiol FJ, Alex V, Arlinson N, Amorim PHA, Amrutkar A, Anand G, Andermatt S, Arbel T, Arbelaez P, Avery A, Azmat M, Pranjali B, Bai W, Banerjee S, Barth B, Batchelder T, Batmanghelich K, Battistella E, Beers A, Belyaev M, Bendszus M, Benson E, Bernal J, Bharath HN, Biros G, Bisdas S, Brown J, Cabezas M, Cao S, Cardoso JM, Carver EN, Casamitjana A, Castillo LS, Catà M, Cattin P, Cerigues A, Chagas VS, Chandra S, Chang YJ, Chang S, Chang K, Chazalon J, Chen S, Chen W, Chen JW, Chen Z, Cheng K, Choudhury AR, Chylla R, Clérigues A, Coleman S, Colmeiro RGR, Combalia M, Costa A, Cui X, Dai Z, Dai L, Daza LA, Deutsch E, Ding C, Dong C, Dong S, Dudzik W, Eaton-Rosen Z, Egan G, Escudero G, Estienne T, Everson R, Fabrizio J, Fan Y, Fang L, Feng X, Ferrante E, Fidon L, Fischer M, French AP, Fridman N, Fu H, Fuentes D, Gao Y, Gates E, Gering D, Gholami A, Gierke W, Glocker B, Gong M, González-Villá S, Grosgeat T, Guan Y, Guo S, Gupta S, Han WS, Han IS, Harmuth K, He H, Hernández-Sabaté A, Herrmann E, Himthani N, Hsu W, Hsu C, Hu X, Hu X, Hu Y, Hu Y, Hua R, Huang TY, Huang W, Van Huffel S, Huo Q, Hu V, Iftekaruddin KM, Isensee F, Islam M, Jackson AS, Jambawalikar SR, Jesson A, Jian W, Jin P, Jose VJM, Jungo A, Kainz B, Kamnitsas K, Kao PY, Karmawat A, Kellermeier T, Kermi A, Keutzer K, Khadir MT, Khened M, Kickingereder P, Kim G, King N, Knapp H, Knecht U, Kohli L, Kong D, Kong X, Koppers S, Kori A, Krishnamurthi G, Krivov E, Kumar P, Kushibar K, Lachinov D, Lambrou T, Lee J, Lee C, Lee Y, Lee M, Lefkovičs S, Lefkovičs L, Levitt J, Li T, Li H, Li W, Li H, Li X, Li Y, Li H, Li Z, Li X, Li Z, Li X, Li W, Lin ZS, Lin F, Lio P, Liu C, Liu B, Liu X, Liu M, Liu J, Liu L, Liado X, Lopez MM, Lorenzo PR, Lu Z, Luo L, Luo Z, Ma J, Ma K, Mackie T, Madabushi A, Mahmoudi I, Maier-Hein KH, Maji P, Mammn C, Mang A, Manjunath BS, Marcinkiewicz M, McDonagh S, McKenna S, McKinley R, Mehl M, Mehta S, Mehta R, Meier R, Meinel C, Merhof D, Meyer C, Miller R, Mitra S, Moiyadi A, Molina-Garcia D, Monteiro MAB, Mrukwa G, Myronenko A, Nalepa J, Ngo T, Nie D, Ning H, Niu C, Nuechterlein NK, Oermann E, Oliveira A, Oliveira DDC, Oliver A, Osman AFI, Ou Y-N, Ourselin S, Paragios N, Park MS, Paschke B, Pauloski JG, Pawar K, Pawlowski N, Pei L, Peng S, Pereira SM, Perez-Beteta J, Perez-Garcia VM, Pezold S, Pham B, Phophalia A, Piella G, Pillai GN, Piraud M, Pivov M, Popli A, Pound MP, Pourreza R, Prasanna P, Prkowska V, Pridmore TP, Puch S, Puybareau É, Qian B, Qiao X, Rajchl M, Rane S, Rebsamen M, Ren H, Ren X, Revanuru K, Rezaei M, Rippel O, Rivera LC, Robert C, Rosen B, Rueckert D, Safwan M, Saleem M, Salvi J, Sanchez I, Sánchez I, Santos HM, Sartor E, Schellingerhout D, Scheufeke K, Scott MR, Scussel AA, Sedlar S, Serrano-Rubio JP, Shah NJ, Shah N, Shaikh M, Shankar BU, Shboul Z, Shen H, Shen D, Shen L, Shen H, Shenoy V, Shi F, Shin HE, Shu H, Sima D, Sinclair M, Smedby O, Snyder JM, Soltaninejad M, Song G, Soni M, Stawiaski J, Subramanian S, Sun L, Sun R, Sun J, Sun K, Sun Y, Sun G, Sun S, Suter YR, Szilagyi L, Talbar S, Tao D, Tao D, Teng Z, Thakur S, Thakur MH, Tharakan S, Tiwari P, Tochon G, Tran T, Tsai YM, Tseng KL, Tuan TA, Turlapov V, Tustison N, Vakalopoulou M, Valverde S, Vanguri R, Vasiliev E, Ventura J, Vera L, Vercauteren T, Verrastro CA, Vidyaratne L, Vilaplana V, Vivekanandan A, Wang G, Wang Q, Wang CJ, Wang W, Wang D, Wang R, Wang Y, Wang C, Wang G, Wen N, Wen X, Weninger L, Wick W, Wu S, Wu Q, Wu Y, Xia Y, Xu Y, Xu X, Xu P, Yang TL, Yang X, Yang HY, Yang J, Yang H, Yang G, Yao H, Ye X, Yin C, Young-Moxon B, Yu J, Yue X, Zhang S, Zhang A, Zhang K, Zhang X, Zhang L, Zhang X, Zhang Y, Zhang L, Zhang J, Zhang X, Zhang T, Zhao S, Zhao Y, Zhao X, Zhao L, Zheng Y, Zhong L, Zhou C, Zhou X, Zhou F, Zhu H, Zhu J, Zhuge Y, Zong W, Kalpathy-Cramer J, Farahani K, Davatzikos C, van Leemput K, Menze B. Identifying the best machine learning algorithms for brain tumor segmentation, progression assessment, and overall survival prediction in the BRATS challenge. *bioRxiv* publication, 2018;124. Available at: <http://arxiv.org/abs/1811.02629>. Accessed April 23, 2019
- [4] Ben-Hur A, Weston J. A user's guide to support vector machines. In: Carugo O, Eisenhaber F, editors. *Data mining techniques for the life sciences*. Totowa: Humana Press, 2010. p. 223–39.
- [5] Biesiada J, Duch W, Duch W. Feature selection for high-dimensional data—a Pearson redundancy based filter. In: *Computer recognition systems 2*, 2008. Available at: https://doi.org/10.1007/978-3-540-75175-5_30. Accessed October 18, 2007.
- [6] Bzdok D, Altman N, Krzywinski M. Statistics versus machine learning. *Nat Methods* 2018;15:233–4.
- [7] Cardoso-Cruz H, Sousa M, Vieira JB, Lima D, Galhardo V. Prefrontal cortex and mediadorsal thalamus reduced connectivity is associated with spatial working memory impairment in rats with inflammatory pain. *PAIN* 2013;154:2397–406.
- [8] Cauda F, Palermo S, Costa T, Torta R, Duca S, Vercelli U, Geminiani G, Torta DME. Gray matter alterations in chronic pain: a network-oriented meta-analytic approach. *Neuroimage Clin* 2014;4:676–86.
- [9] Danylyuk H, Andrews J, Kesarwani R, Seres P, Broad R, Wheatley BM, Sankar T. The thalamus in trigeminal neuralgia: structural and metabolic abnormalities, and influence on surgical response. *BMC Neurol* 2021;21:290.
- [10] DeKraaker J, Palomero-Gallagher N, Kedo O, Ladbon-Bernasconi N, Muenzing SE, Axer M, Amunts K, Khan AR, Bernhardt BC, Evans AC. Evaluation of surface-based hippocampal registration using ground-truth subfield definitions. *eLife* 2023;12:RP88404.
- [11] Destrieux C, Fischl B, Dale A, Halgren E. Automatic parcellation of human cortical gyri and sulci using standard anatomical nomenclature. *Neuroimage* 2010;53:1–15.
- [12] Di Stefano G, Maarbjerg S, Truini A. Trigeminal neuralgia secondary to multiple sclerosis: from the clinical picture to the treatment options. *J Headache Pain* 2019;20:20.
- [13] Erickson BJ, Korfiatis P, Akkus Z, Kline TL. Machine learning for medical imaging. *Radiographics* 2017;37:505–15.
- [14] Erpelding N, Moayeddi M, Davis KD. Cortical thickness correlates of pain and temperature sensitivity. *PAIN* 2012;153:1602–9.
- [15] Ferraro D, Plantone D, Morselli F, Dallari G, Simone AM, Vitetta F, Sola P, Primiano G, Nociti V, Pardini M, Mirabella M, Vollono C. Systematic assessment and characterization of chronic pain in multiple sclerosis patients. *Neurol Sci* 2018;39:445–53.
- [16] FreeSurfer. n.d. Available at: <https://surfer.nmr.mgh.harvard.edu/>. Accessed August 21, 2023.
- [17] GBD 2016 Disease and Injury Incidence and Prevalence Collaborators. Global, regional, and national incidence, prevalence, and years lived with disability for 328 diseases and injuries for 195 countries, 1990–2016: a systematic analysis for the Global Burden of Disease Study 2016. *Lancet* 2017;390:1211–59.
- [18] Haider L, Simeonidou C, Steinberger G, Hametner S, Grigoriadis N, Deretzi G, Kovacs GG, Kutzelnigg A, Lassmann H, Frischer JM. Multiple sclerosis deep grey matter: the relation between demyelination, neurodegeneration, inflammation and iron. *J Neurol Neurosurg Psychiatry* 2014;85:1386–95.
- [19] Headache Classification Committee of the International Headache Society (IHS) The International Classification of Headache Disorders, 3rd edition. *Cephalalgia* 2018;38:1–211.
- [20] Herr K, Coyne PJ, Ely E, Gélinas C, Manworen RCB. Pain assessment in the patient unable to self-report: clinical practice recommendations in support of the ASPMN 2019 position statement. *Pain Manag Nurs* 2019;20:404–17.
- [21] Hou AL, Wu JJ, Xing XX, Huo BB, Shen J, Hua XY, Zheng MX, Xu JG. Multivariate pattern analysis in identifying neuropathic pain following brachial plexus avulsion injury: a PET/CT study. *Pain Physician* 2022;25:E147–56.
- [22] Huang T, Lin SH, Malewicz NM, Zhang Y, Zhang Y, Goulding M, LaMotte RH, Ma Q. Identifying the pathways required for coping behaviours associated with sustained pain. *Nature* 2019;565:86–90.
- [23] Hung PSP, Noorani A, Zhang JY, Tohyama S, Laperriere N, Davis KD, Mikulis DJ, Rudzicz F, Hodaie M. Regional brain morphology predicts pain relief in trigeminal neuralgia. *Neuroimage Clin* 2021;31:102706.
- [24] Kawachi I, Lassmann H. Neurodegeneration in multiple sclerosis and neuromyelitis optica. *J Neurol Neurosurg Psychiatry* 2017;88:137–45.
- [25] Kawai K, Kawai AT, Wollan P, Yawn BP. Adverse impacts of chronic pain on health-related quality of life, work productivity, depression and anxiety in a community-based study. *Fam Pract* 2017;34:656–61.
- [26] Krishnan S, Bigder M, Kaufmann AM. Long-term follow-up of multimodality treatment for multiple sclerosis-related trigeminal neuralgia. *Acta Neurochir (Wien)* 2018;160:135–44.
- [27] Kuhlmann T, Moccia M, Coetzee T, Cohen JA, Correale J, Graves J, Marrie RA, Montalban X, Yong VW, Thompson AJ, Reich DS; International Advisory Committee on Clinical Trials in Multiple Sclerosis, Amato MP, Banwell B, Barkhof F, Chataway J, Chitnis T, Comi G, Derfuss T, Finlayson M, Goldman M, Green A, Hellwig K, Kos D, Miller A, Mowry E, Oh J, Salter A, Sormani MP, Tintore M, Tremlett Helen, Trojano M, van der Walt A, Vukusic S, Waubant E. Multiple sclerosis progression: time for a new mechanism-driven framework. *Lancet Neurol* 2023;22:78–88.
- [28] Kurtzke JF. Rating neurologic impairment in multiple sclerosis: an expanded disability status scale (EDSS). *Neurology* 1983;33:1444–52.
- [29] Kutzelnigg A, Lucchinetti CF, Stadelmann C, Brück W, Rauscher H, Bergmann M, Schmidbauer M, Parisi JE, Lassmann H. Cortical demyelination and diffuse white matter injury in multiple sclerosis. *Brain* 2005;128(pt 11):2705–12.
- [30] Lassmann H. Multiple sclerosis pathology. *Cold Spring Harb Perspect Med* 2018;8:a028936.
- [31] Latypov TH, So MC, Hung PSP, Tsai P, Walker MR, Tohyama S, Tawfik M, Rudzicz F, Hodaie M. Brain imaging signatures of neuropathic facial pain derived by artificial intelligence. *Sci Rep* 2023;13:10699.
- [32] Liu X, Gu L, Liu J, Hong S, Luo Q, Wu Y, Yang J, Jiang J. MRI study of cerebral cortical thickness in patients with herpes zoster and postherpetic neuralgia. *J Pain Res* 2022;15:623–32.

- [33] Maeda Y, Kettner N, Kim J, Kim H, Cina S, Malatesta C, Gerber J, McManus C, Libby A, Mezzacappa P, Mawla I, Morse LR, Audette J, Napadow V. Primary somatosensory/motor cortical thickness distinguishes paresthesia-dominant from pain-dominant carpal tunnel syndrome. *PAIN* 2016;157:1085–93.
- [34] Megna R, Petretta M, Assante R, Zampella E, Nappi C, Gaudieri V, Mannarino T, D'Antonio A, Green R, Cantoni V, Arumugam P, Acampa W, Cuocolo A. A comparison among different machine learning pretest approaches to predict stress-induced ischemia at PET/CT myocardial perfusion imaging. *Comput Math Methods Med* 2021;2021:3551756.
- [35] Moayedi M, Weissman-Fogel I, Crawley AP, Goldberg MB, Freeman BV, Tenenbaum HC, Davis KD. Contribution of chronic pain and neuroticism to abnormal forebrain gray matter in patients with temporomandibular disorder. *Neuroimage* 2011;55:277–86.
- [36] Motzkin J, Hiser J, Carroll I, Wolf R, Baskaya M, Koenigs M, Atlas L. Human ventromedial prefrontal cortex lesions enhance expectation-related pain modulation. *Cortex* 2023;166:188–206. Accessed June 09, 2023.
- [37] van Munster CEP, Jonkman LE, Weinstein HC, Uitdehaag BMJ, Geurts JJG. Gray matter damage in multiple sclerosis: impact on clinical symptoms. *Neuroscience* 2015;303:446–61.
- [38] Nguyen MH, de la Torre F. Optimal feature selection for support vector machines. *Pattern Recognition* 2010;43:584–91.
- [39] Noble WS. What is a support vector machine? *Nat Biotechnol* 2006;24:1565–7.
- [40] Noorani A, Hung PSP, Zhang JY, Sohng K, Laperrriere N, Moayedi M, Hodaie M. Pain relief reverses hippocampal abnormalities in trigeminal neuralgia. *J Pain* 2022;23:141–55.
- [41] Ong WY, Stohler CS, Herr DR. Role of the prefrontal cortex in pain processing. *Mol Neurobiol* 2019;56:1137–66.
- [42] Panta SR, Wang R, Fries J, Kalyanam R, Speer N, Banich M, Kiehl K, King M, Milham M, Wager TD, Turner JA, Plis SM, Calhoun VD. A tool for interactive data visualization: application to over 10,000 brain imaging and phantom MRI data sets. *Front Neuroinform* 2016;10:9.
- [43] Parise M, Kubo TTA, Doring TM, Tukamoto G, Vincent M, Gasparetto EL. Cuneus and fusiform cortices thickness is reduced in trigeminal neuralgia. *J Headache Pain* 2014;15:17.
- [44] Racke MK, Frohman EM, Frohman T. Pain in multiple sclerosis: understanding pathophysiology, diagnosis, and management through clinical vignettes. *Front Neurol* 2022;12:799698.
- [45] Raschka S. MLxtend: providing machine learning and data science utilities and extensions to Python's scientific computing stack. *J Open Source Softw* 2018;3:638.
- [46] Rashidi P, Edwards DA, Tighe PJ. Primer on machine learning: utilization of large data set analyses to individualize pain management. *Curr Opin Anaesthesiol* 2019;32:653–60.
- [47] scikit-learn: machine learning in Python—scikit-learn 1.3.0 documentation. n.d. Available at: <https://scikit-learn.org/stable/index.html>. Accessed August 21, 2023.
- [48] Selvarajah D, Wilkinson ID, Fang F, Sankar A, Davies J, Boland E, Harding J, Rao G, Gandhi R, Tracey I, Tesfaye S. Structural and functional abnormalities of the primary somatosensory cortex in diabetic peripheral neuropathy: a multimodal MRI study. *Diabetes* 2019;68:796–806.
- [49] Shankar Kikkeri N, Nagalli S. Trigeminal neuralgia. In: *StatPearls*. Treasure Island: StatPearls Publishing, 2023. Available at: <http://www.ncbi.nlm.nih.gov/books/NBK554486/>. Accessed October 6, 2023.
- [50] Shirvalkar P, Prosky J, Chin G, Ahmadipour P, Sani OG, Desai M, Schmitgen A, Dawes H, Shanchei MM, Starr PA, Chang EF. First-in-human prediction of chronic pain state using intracranial neural biomarkers. *Nat Neurosci* 2023;26:1090–9.
- [51] Solaro C, Brichetto G, Amato MP, Cocco E, Colombo B, D'Aleo G, Gasperini C, Ghezzi A, Martinelli V, Milanese C, Patti F, Trojano M, Verdun E, Mancardi GL; PaIMS Study Group. The prevalence of pain in multiple sclerosis: a multicenter cross-sectional study. *Neurology* 2004;63:919–21.
- [52] Su Q, Song Y, Zhao R, Liang M. A review on the ongoing quest for a pain signature in the human brain. *Brain Sci Adv* 2019;5:274–87.
- [53] Taylor JR, Williams N, Cusack R, Auer T, Shafto MA, Dixon M, Tyler LK; Cam-CAN, Henson RN. The Cambridge Centre for Ageing and Neuroscience (Cam-CAN) data repository: structural and functional MRI, MEG, and cognitive data from a cross-sectional adult lifespan sample. *Neuroimage* 2017;144(pt B):262–9.
- [54] Timmler S, Simons M. Grey matter myelination. *Glia* 2019;67:2063–70.
- [55] Tomassy GS, Berger DR, Chen HH, Kasthuri N, Hayworth KJ, Vercelli A, Seung HS, Lichtman JW, Arlotta P. Distinct profiles of myelin distribution along single axons of pyramidal neurons in the neocortex. *Science* 2014;344:319–24.
- [56] Uddin LQ, Yeo BTT, Spreng RN. Towards a universal taxonomy of macro-scale functional human brain networks. *Brain Topogr* 2019;32:926–42.
- [57] Vaculik MF, Noorani A, Hung PSP, Hodaie M. Selective hippocampal subfield volume reductions in classic trigeminal neuralgia. *Neuroimage Clin* 2019;23:101911.
- [58] Winkler AM, Greve DN, Bjuland KJ, Nichols TE, Sabuncu MR, Håberg AK, Skranes J, Rimol LM. Joint analysis of cortical area and thickness as a replacement for the analysis of the volume of the cerebral cortex. *Cereb Cortex* 2018;28:738–49.
- [59] You HJ, Lei J, Pertovaara A. Thalamus: the "promoter" of endogenous modulation of pain and potential therapeutic target in pathological pain. *Neurosci Biobehav Rev* 2022;139:104745.
- [60] Zakrzewska JM, Wu J, Mon-Williams M, Phillips N, Pavitt SH. Evaluating the impact of trigeminal neuralgia. *PAIN* 2017;158:1166–74.